30 December 2019

Dropsonde Data Quality Report

Organization of Tropical East Pacific Convection
OTREC (2019)

Holger Vömel, Mack Goodstein, Laura Tudor, Jacquelyn Witte
Earth Observing Laboratory
National Center for Atmospheric Research
Boulder, CO

Earth Observing Laboratory
In situ Sensing Facility

NATIONAL CENTER FOR ATMOSPHERIC RESEARCH
P. O. Box 3000
BOULDER, COLORADO 80307-3000

The dropsonde data for this project were quality controlled and are maintained by the Earth Observing Laboratory at the National Center for Atmospheric Research (NCAR). The National Center for Atmospheric Research is managed by the University Corporation for Atmospheric Research and sponsored by the National Science Foundation.
If information or plots from this document are used for publication or presentation purposes, please provide appropriate acknowledgement to NCAR/EOL and NSF and refer to the citation listed below. Please feel free to contact the authors for further information.

Contact:
Holger Vömel (voemel@ucar.edu)

Dropsonde Operators:
Mack Goodstein (NCAR)
Laura Tudor (NCAR)
Holger Vömel (NCAR)

Real-Time Dropsonde Quality Control:
Jose Martinez-Claros (New Mexico Tech)
Ana Juracic (New Mexico Tech)
Vijit Maithel (U. Wisconsin)
Stipo Sentic (New Mexico Tech)
Justin Whitaker (Colorado State University)

Campaign Websites:
OTREC home page:
https://www.eol.ucar.edu/field_projects/otrec
AVAPS dropsondes home page:
https://www.eol.ucar.edu/observing_facilities/avaps-dropsonde-system

To refer to this data set or report, please include the following citation:

UCAR/NCAR - Earth Observing Laboratory, Voemel, H. 2019. NCAR/EOL AVAPS Dropsonde QC Data. Version 1.0. UCAR/NCAR - Earth Observing Laboratory. https://doi.org/10.26023/EHRT-TN96-9W04. Accessed 10 Jan 2020.

Document Version Control

Version	Date	Author	Change Description
1.0	30 Dec 2019	H. Vömel	Initial Data Release

1 Table of Contents

2 Dataset overview

The Organization of Tropical East Pacific Convection (OTREC) field campaign studies the distribution of deep atmospheric convection in the tropical East Pacific and tries to answer a number of scientific questions, such as: What determines the distribution of deep atmospheric convection in this region, including especially its day-to-day variability? Why does higher rainfall occur over lower sea surface temperatures? Why do easterly waves form and/or intensify in the Far East Pacific off the coasts of Central America and Colombia. To address these questions, OTREC conducted a two-month long field campaign of NSF/NCAR Gulfstream-V aircraft observations using the NCAR Airborne Vertical Atmospheric Profiling System (AVAPS) dropsondes and the HIAPER Cloud Radar (HCR). In addition, ground based remote sensing observations of integrated precipitable water vapor and balloon borne profiling at two sites in Costa Rica and one site in Colombia were conducted. This data quality report details the observations using the NCAR AVAPS dropsondes.

Twenty-two research flights were conducted between 7 Aug and 2 Oct 2019, during which 648 dropsondes were successfully released.

Two different flight track patterns had been defined prior to the campaign, originating in Liberia, Costa Rica, which are shown in Figure 1. Each nominal flight pattern consisted of eight legs with four sounding locations each for a total of 32 scheduled soundings per flight.

On some flights, the eastern B1 pattern was modified such that the dropsonde locations were serviced in a N/S direction rather than E/W direction. On several flights, one additional dropsonde was launched in the Panama Bight.

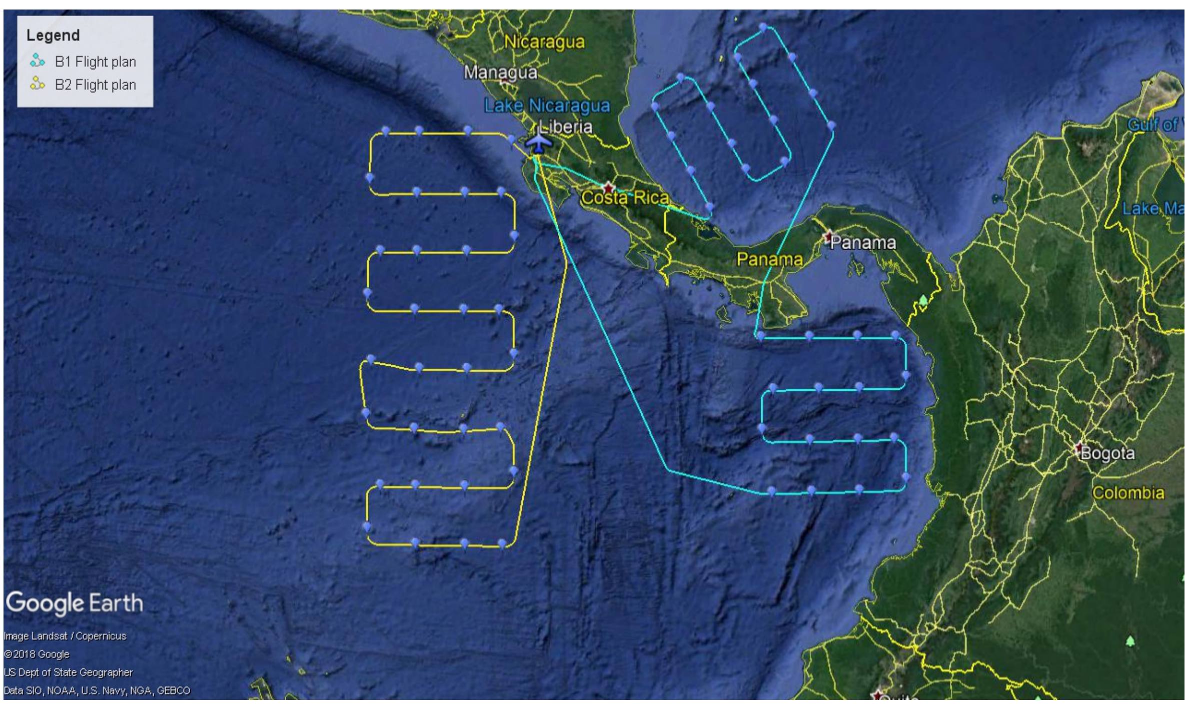

Figure 1: B1 (blue) and B2 (yellow) flight patterns and typical dropsonde locations.

Research flight six on 18 August 2019 (Figure 2, left panel) deviated from the regular pattern, since this flight was conducted in coordination with a NOAA P-3 research flight, which took place at the same time and also originated from Liberia.

Research flight seventeen on 25 September 2019 (Figure 2, right panel) extended the Eastern Pacific lawn mower pattern to the south and skipped most of the Caribbean drop locations.

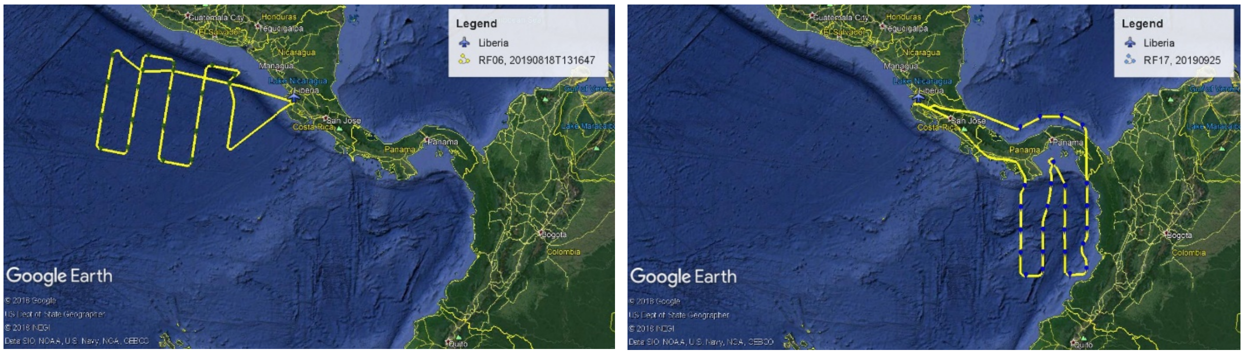

Figure 2: Left: Flight pattern during RF06 on 18 August 2019. Right: Flight pattern during RF017 on 25 September 2019.

The tracks for all 22 flights and the locations of all dropsonde releases are shown in Figure 3.

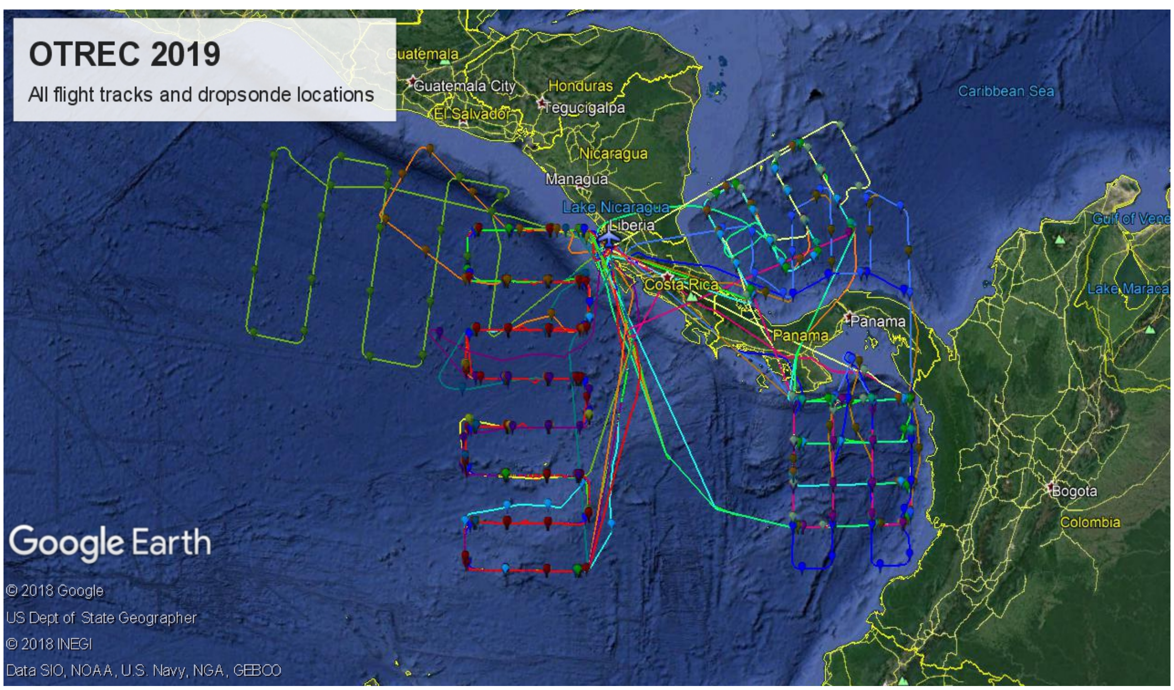

Figure 3: All flights tracks and all dropsonde locations during OTREC.

Table 2 provides an overview over the performance of the dropsonde system as whole. In total, 657 sondes were released from the aircraft. Nine soundings failed at launch and provided no data. In eight soundings, the telemetry stopped before the sonde reached the ground. In four additional sounding, the GPS unit failed and provided no winds. The issues encountered are discussed in more detail below.

The overall success rate of the dropsonde system for this campaign is at 96.8% using the NCAR NRD41 dropsonde.

Table 1 provides an overview over all dropsondes, which were released during OTREC. The B1 and B2 pattern had been designed with 8 legs of 4 sondes for a total of 32 drops per flight. Some flights did not achieve the scheduled number of drops. Reasons were changes in the flight plan, weather related, failure of the dropsonde launcher, or aircraft problems.

Table 2 provides an overview over the performance of the dropsonde system as whole. In total, 657 sondes were released from the aircraft. Nine soundings failed at launch and provided no data. In eight soundings, the telemetry stopped before the sonde reached the ground. In four additional sounding, the GPS unit failed and provided no winds. The issues encountered are discussed in more detail below.

The overall success rate of the dropsonde system for this campaign is at 96.8% using the NCAR NRD41 dropsonde.

Table 1: Overview over all successful sonde releases during OTREC.

Flight	Pattern	Date	# of Soundings
RF01	B2	07 Aug	31
RF02	B1	11 Aug	32
RF03	B2	12 Aug	31
RF04	B1	16 Aug	32
RF05	B2	17 Aug	30
RF06	NOAA	18 Aug	20
RF07	B1	22 Aug	30
RF08	B2	23 Aug	29
RF09	B1	25 Aug	24
RF10	B1	03 Sep	32
RF11	B2	04 Sep	21
RF12	B1	09 Sep	32
RF13	B1	17 Sep	29
RF14	B2	21 Sep	34
RF15	B1	22 Sep	32
RF16	B2	24 Sep	33
RF17	B1	25 Sep	25
RF18	B2	27 Sep	32
RF19	B2	28 Sep	32
RF20	B2	30 Sep	32
RF21	B2	01 Oct	31
RF22	B2	02 Oct	24

Table 2: Overview of the dropsonde system performance.

	# of Sondes	Percent
Total number of sondes released	657	100
Successful releases	648	98.6
Complete thermodynamic profiles to the ground	640	97.4
Complete wind profiles to the ground	636	96.8

3 Dropsonde sounding system

The NCAR dropsonde system deployed in OTREC used the automated dropsonde launcher for the NSF/NCAR G-V and the newly developed NCAR Research Dropsonde model NRD41.

The NRD41 dropsonde uses the pressure, temperature, and humidity sensor of the Vaisala RS41 radiosonde and employs an improved version of the GPS, telemetry, and parachute release system of the previous NRD94 dropsonde, which had been in use between 2011 and 2018. It has been successfully tested during the Southern Ocean Clouds, Radiation, Aerosol Transport Experimental Study (SOCRATES) field campaign in January and February of 2018.

The larger version of this dropsonde, the RD41 dropsonde, was developed in parallel to the NRD41 and has been introduced into operational service by NOAA and the Air Force in 2018.

All dropsonde humidity sensors were reconditioned prior to loading sondes into the dropsonde launcher. This process, which is unique to the xRD41 dropsondes, reduces the potential of humidity contamination to a minimum and assures the best measurement performance throughout the entire altitude and temperature range of the profiles.

The AVAPS LabVIEW based software system receives and stores data from the dropsondes, the aircraft data system, and controls and monitors the AVAPS launch system.

The automated dropsonde launcher was installed in the baggage compartment of the NCAR G-V research aircraft and was remotely controlled from the AVAPS station onboard the aircraft. This allowed dropsonde operations at the service ceiling of the aircraft, with a maximum drop altitude of 14.9 km, while providing easy access to the launcher in case of malfunction.

Profile data were transmitted after the completion of each drop to the OTREC operations center at Playa Panama, Costa Rica, where OTREC scientific staff controlled the quality of each sounding using the Atmospheric Sounding Processing ENvironment (ASPEN) software package. The quality controlled data of all soundings that did not raise any quality concerns were transmitted to the Global Telecommunications System (GTS) of the WMO, which allowed data centers assimilating these data for analysis and forecasting.

During the first half of the campaign, a small number of sondes did not launch properly and became stuck in the launcher. These sondes had to be removed manually and new sondes had to be loaded before a replacement sonde could be released. The launch problems were exacerbated during RF11 on 4 Sep 2019, when the launcher stopped releasing sondes and the flight had to be aborted prematurely after the release of only 21 sondes. Maintenance of the launcher uncovered three broken springs, which had to be replaced and which led to an additional delay in the flight schedule. We speculate that between three and six of the failed dropsondes were damaged at launch as a result of the launcher damage.

After its repair, the dropsonde launcher performed as expected and no further dropsonde release problems were encountered.

4 Quality control procedures

4.1 Standard quality control

Standard quality control in near real time and as part of the final data QC is based on the algorithms implemented in the ASPEN software. The following quality checks, corrections, and calculations are performed:

- Removal of outliers and suspect data points in pressure, temperature, humidity, zonal and meridional wind, latitude, and longitude

- Removal of data between release from the aircraft and equilibration with atmospheric conditions
- Dynamic correction to account for the lag of the NRD41 temperature sensor using the appropriate coefficients for the NRD41 dropsondes
- Dynamic correction to account for the sonde inertia in the determination of the wind profile using the appropriate parameters for the NRD41 dropsondes
- Smoothing of pressure, temperature, humidity, zonal and meridional wind
- Recomputing of wind speed and wind direction after smoothing of the wind components
- Extrapolation of the last reported pressure reading to a surface pressure value (where possible), based on the fall rate of the sonde
- Recalculation of the geopotential height from the surface to the top of the profile
- Computing a vertical wind speed component

During each flight, scientific staff processed each sounding as they were transmitted from the aircraft and generated the appropriate FM 37 TEMP DROP and 3 09 053 BUFR messages using ASPEN. All soundings that were considered of high enough quality were sent to the WMO GTS for use in forecast and climate models.

This campaign used the new NRD41 dropsonde, which has a faster temperature sensor and faster RH sensor than the older NRD94 sondes. This has been considered in the final dropsonde QC by changing the ASPEN QC parameters for these two sensors. The equilibration time for the temperature and RH sensor has been adjusted to 20 s, and the smoothing wavelength for both parameters has been adjusted to 5 s.

4.2 Custom quality control

4.2.1 Pressure corrections

The pressure sensor of the NRD41 dropsonde is known to have a small bias. This sensor bias is measured during the production of the dropsondes and a correction is stored in the sonde to minimize the bias during observation. In addition, the AVAPS dropsondes launcher contains a high-quality reference pressure sensor, which measures the pressure inside the dropsonde launcher. This reference pressure was used to further reduce any residual bias of the NRD41 pressure sensor.

The statistics of the residual pressure bias measured inside the launcher is shown in Figure 4. The median pressure offset is 0.35 hPa and the standard deviation 0.17 hPa. These measurements were used to correct the dropsonde pressure readings during flight. The surface pressures reported by the dropsondes are expected to have only minimal systematic biases.

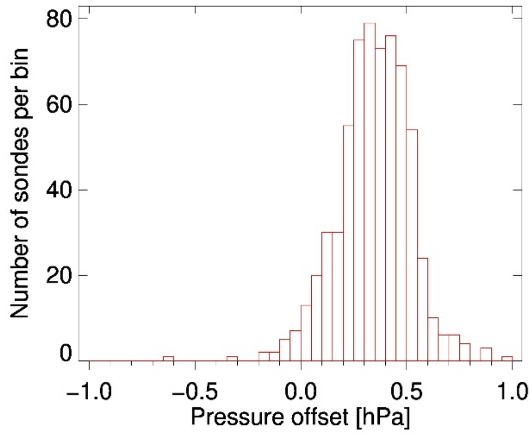

Figure 4: Pressure offset between the dropsonde and the reference sensor before launch.

During OTREC, most sondes exhibited a small pressure measurement issue. For reasons currently unknown, the dropsondes occasionally repeated a reported pressure measurement. This happened up to 20 times per sounding and in a few cases more frequently. While this is barely noticeable in any vertical profile, it did lead to additional noise in the calculated vertical fall rate. In post processing, these repeated pressure readings were interpolated and the fall rates were recalculated excluding these values. Only pressure readings had to be corrected. Temperature and relative humidity readings did not show any artificial repetition of measurements.

4.2.2 Relative humidity

The RH sensor on the xRD41 dropsondes should be reconditioned prior to launch. The sondes store the information, whether the reconditioning was successful. Therefore we were able to verify that all sondes were properly reconditioned prior to take off before each flight. Any contamination in the sensor material was removed and the relative humidity sensors were expected to perform with negligible calibration drift.

The time response of the NRD41 relative humidity sensor is a few 10ths of seconds near the surface and nearly one minute at flight level of the G-V. A correction for this response time lag has not yet been implemented in ASPEN but was applied in post processing. The effect of this correction is noticeable at altitudes above approximately 11.5 km and strongly increases the reported relative humidity near the top of the profiles.

Figure 5 shows the average relative humidity profiles for all OTREC soundings before the time lag correction (red) and after time lag correction (blue). The effect of the time lag correction becomes significant only above 11.5 km, where the time constant of the sensor becomes very large, and where the reported profile shows a consistent vertical gradient. At 13 km, the time lag correction increases the relative humidity from an average value of 24% to 48%, i.e. by a factor of two. Ice saturation is at about 55% relative humidity (over liquid), which implies that the time lag corrected relative humidity measurements are more realistic for tropical measurements.

We removed the first 20 s of the relative humidity and temperature profiles, while the sensors are equilibrating to the ambient environment. Lacking any validating observations, some uncertainty in the relative humidity at the top of the profile remains and we would estimate that the layer 500 m below the aircraft should be treated with caution.

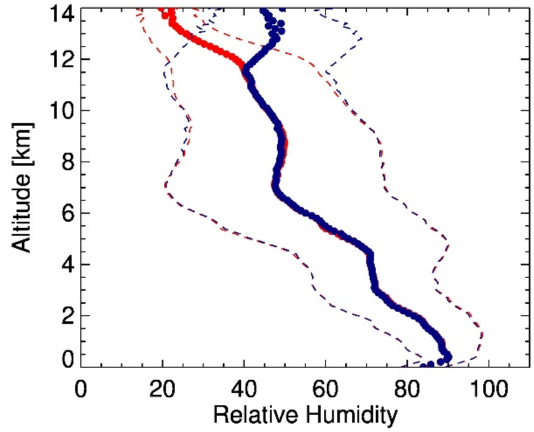

Figure 5: Mean relative humidity profile for all OTREC soundings. The average of the uncorrected relative humidity is shown in red, the average of the time lag corrected relative humidity is shown in blue. The standard deviation for each is shown as dashed lines

4.2.3 Launcher related problems

The launcher malfunction during the first half of the campaign led to damage in several sondes during the launch process. Indications of this damage was an internal sonde temperature much colder than normal. In four sondes, listed in Table 3, this damage also led to a slower response of the atmospheric temperature sensor. The slower temperature response was noticeable only in the atmospheric equilibration after release, but not in the middle and lower troposphere. In these four profiles, the equilibration time was significantly extended to remove any artifacts near the top of the profile.

Table 3: Soundings with slower equilibration after launch

#	Research Flight	Sounding
1	RF03	20190812_142104
2	RF07	20190822_172906
3	RF07	20190822_181226
4	RF08	20190823_164923

Nine soundings failed at launch, which means either the telemetry stream stopped at launch, or the sondes reported a failure of the sensor modules at launch. We estimate that at least three and up to six of the failed sondes at launch, may have been damaged by the launcher malfunction, which was not appreciated during the campaign. After repair of the launcher, no further launcher related problems were observed and only one more sonde stopped working at the moment of launch.

4.2.4 Parachute performance

The parachute performed as expected in 98.2% of all soundings. In two sondes (Table 4), the parachutes apparently did not function properly throughout the sounding and the sonde fell significantly faster than normal. The failure of the first sonde is likely related to the launcher malfunction. The failure of the second fast fall is less clear. In both cases the estimation of the surface pressure is low biased and the temperature profile may be biased as well.

Table 4: Fast fall soundings

#	Research Flight	Sounding
1	RF06	20190818_175247
2	RF19	20190928_153516

Eight soundings (Table 5) experienced late parachute opening. In these soundings the sonde was initially falling in an undefined orientation and the PTU measurements may have been negatively affected until the parachute properly opened. These data were removed where needed to eliminate biased observations.

Table 5: Partial fast fall and altitude of normal parachute performance

#	Research Flight	Sounding	Altitude of normal parachute operation [km]
1	RF04	20190816_150109	12.1
2	RF07	20190822_163810	12.8
3	RF08	20190823_140333	3.3*
4	RF08	20190823_141152	11.4
5	RF12	20190909_171941	11.9
6	RF12	20190909_182803	12.8
7	RF12	20190909_184131	11.7
8	RF14	20190921_135338	11.4

*) Temperature and relative humidity were set to missing above 11.7 km, GPS wind and altitude were set to missing above 12.5 km and additionally smoothed above 3.51 km .

Sounding 20190822_172237 on RF07 experienced a slightly faster than normal fall rate down to 400 m above ground. All parameters are normal and the sounding was processed normally. Nevertheless, the parachute of this sounding may have been somewhat affected by the launcher malfunction.

Six soundings (Table 6) had a fall rate that was slightly but consistently slower than the expected fall rate. These sondes likely suffered some damage by the malfunctioning launcher, which increased the drag coefficient. The GPS performance was not affected by this damage; however, the performance of the temperature sensor after launch was affected in three soundings. Vertical velocities derived from these sondes should be treated with caution.

Table 6: Sondes falling slower than expected

#	Research Flight	Sounding	Other symptoms
1	RF01	20190807_152431	None
2	RF03	20190812_142104	Slow temperature equilibration after launch above 11.6 km
3	RF06	20190818_175609	Sonde data were lost prematurely at 8.5 km
4	RF07	20190822_172906	Slow temperature equilibration after launch above 10.8 km
5	RF07	20190822_184452	None
6	RF08	20190823_161835	None

4.2.5 GPS performance

The GPS unit in the dropsondes operated properly in 95% of all soundings, i.e. the reported uncertainty of the GPS was around 0.2 m/s in the lower part of the profile and around 0.4 m/s in the upper part of the profile.

Twenty-eight soundings (Table 7) had a degraded performance with an uncertainty of 0.6 m/s in the lower part and up to 1.5 m/s in the upper part of the profile. ASPEN had been configured to remove the wind measurements under these conditions, which had been noticed in the real time processing of these sounding. In post processing, we increased the thresholds for the affected soundings, making recovering the wind measurements that had been rejected in real time.

In three soundings (Table 8), the GPS module failed completely.

Table 7: Soundings with degraded GPS performance. The reported speed uncertainty is reported by the GPS module.

#	Research Flight	Sounding	Median speed uncertainty [m/s]
1	RF01	20190807_132644	0.56
2	RF01	20190807_145019	0.53
3	RF01	20190807_154631	0.65
4	RF01	20190807_160956	0.33
5	RF01	20190807_171952	0.61
6	RF02	20190811_160440	0.67
7	RF02	20190811_164355	0.68
8	RF04	20190816_150109	0.57
9	RF04	20190816_170510	0.55
10	RF05	20190817_140439	1.26*
11	RF05	20190817_162052	0.62
12	RF06	20190818_141632	0.29
13	RF06	20190818_175247	0.31
14	RF07	20190822_183825	0.65
15	RF07	20190822_184452	0.67
16	RF08	20190823_140333	0.38
17	RF08	20190823_154727	0.64
18	RF11	20190904_141442	0.6
19	RF12	20190909_162704	0.67
20	RF12	20190909_165246	0.55
21	RF12	20190909_174246	0.56
22	RF13	20190917_155455	0.42
23	RF14	20190921_142030	0.41
24	RF14	20190921_175614	0.41
25	RF15	20190922_145556	0.55

26	RF15	20190922_154415	0.6
27	RF16	20190924_165614	0.59
28	RF19	20190928_153516	0.31

*) In sounding 20190817_140439, the GPS altitude and GPS fall rate were completely wrong. Therefore, the horizontal winds were removed as well for the entire profile.

Table 8: Soundings, where the GPS module failed.

#	Research Flight	Sounding
1	RF03	D20190812_161306.2
2	RF16	D20190924_161135.4
3	RF20	D20190930_151914.2

4.2.6 Temperature performance

All soundings but one showed consistent temperature observations within expected limits. One sounding during RF17 (20190925_154412) shows a warm bias relative to its neighbors as well as to the nearby Nuqui radiosonde 100 km to the ESE, launched 30 min later. This bias varies between 1.0°C and 3.7°C throughout the profile. It also shows a significantly geopotential height error relative to the other sondes. The temperature measurements during calibration and prior to launch were within specifications and we do not have any indication for a possible cause of this bias; yet, this sounding needs to be treated with caution.

5 Data file format

The format follows that defined for the NCAR/EOL/ISF radiosonde NetCDF data files. It is based on the Climate and Forecasting (CF) convention version 1.6 and is compatible with any tool accepting this convention. The data file format is described in Vömel et al. (2018).

The format description can be found at:

Vömel, H., I. Suhr, and G. Granger, 2019, NCAR/EOL/ISF Dropsonde NetCDF Data Files, UCAR/NCAR - Earth Observing Laboratory. https://doi.org/10.26023/54wh-rj45

6 Sounding metrics

6.1 Horizontal drift

Wind speeds during OTREC were generally weak. As a result, the horizontal drift of the dropsondes was relatively small (Figure 6). The mean horizontal distance the dropsondes traveled was 3.8 km and no sonde traveled more than 10 km horizontally.

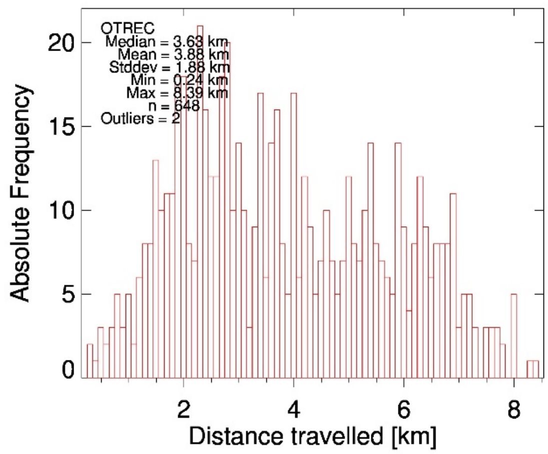

Figure 6: Distance between launch and landing for all dropsondes during OTREC.

6.2 Surface pressure

The surface pressure reported by the sondes is an extrapolation of the last measured air pressure above the surface to sea level using the current fall rate. The surface pressure reported by all sondes, which transmitted to the surface is shown in Figure 7.

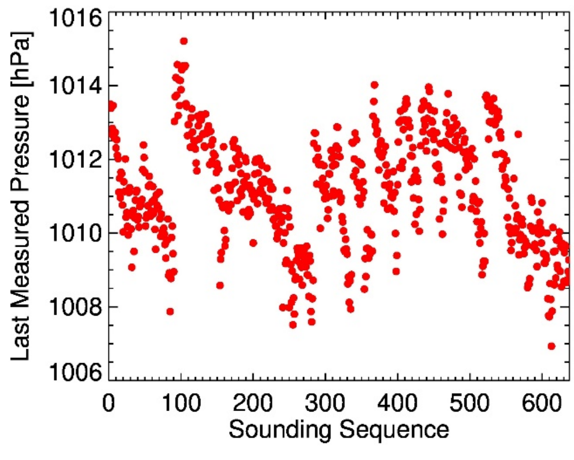

Figure 7: Surface pressure reported by all sondes

6.3 Fall rate

A histogram of the measurement time for soundings with normal parachute performance is shown in Figure 8. Soundings with parachute failure and early telemetry loss are excluded from this plot. The average fall time for all soundings is 14.2 min. The increasing aircraft altitude during each research flight contributes significantly to the width of the distribution. Nevertheless, the consistency of the fall times highlights the quality of the parachute performance of the dropsondes used in OTREC.

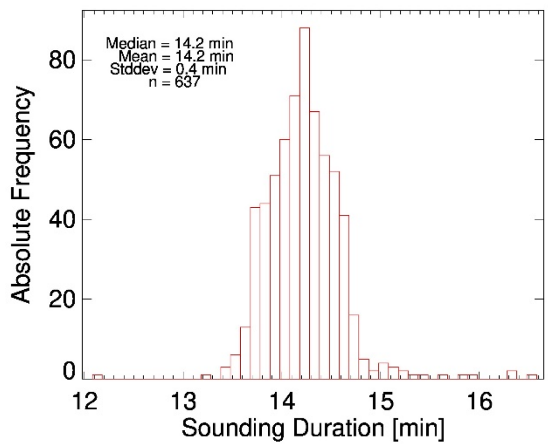

Figure 8: Measurement duration for all dropsonde with normal parachute behavior reaching the surface.

7 Atmospheric observations

7.1 Temperature

The temperature measured by all dropsondes is shown as contour plot in Figure 9. The individual research flights are separated by vertical lines. The temperature at flight level were in the range of -60°C to -70°C and near the surface in the range of 22°C to 29°C.

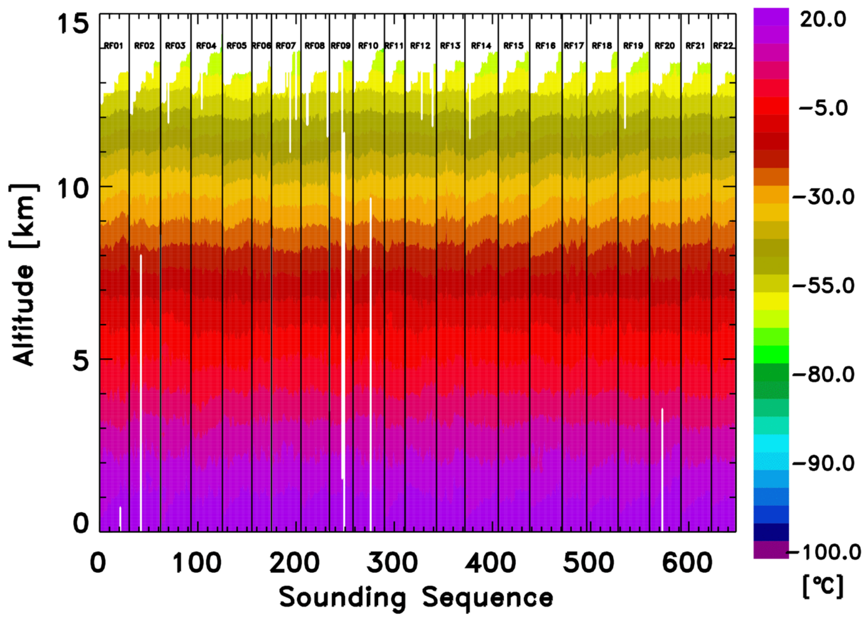

Figure 9: Color contours for all temperature measurements. Missing data are shown in white. All soundings are shown in the sequence in which they were released.

7.2 Relative humidity

Relative humidity measured by all dropsondes is shown in Figure 10. At temperatures below 0°C, relative humidity is expressed as relative humidity over ice instead of the conventional relative humidity over liquid water. Areas near and above saturation in the upper troposphere are periods when the aircraft flew in or above high level cirrus clouds.

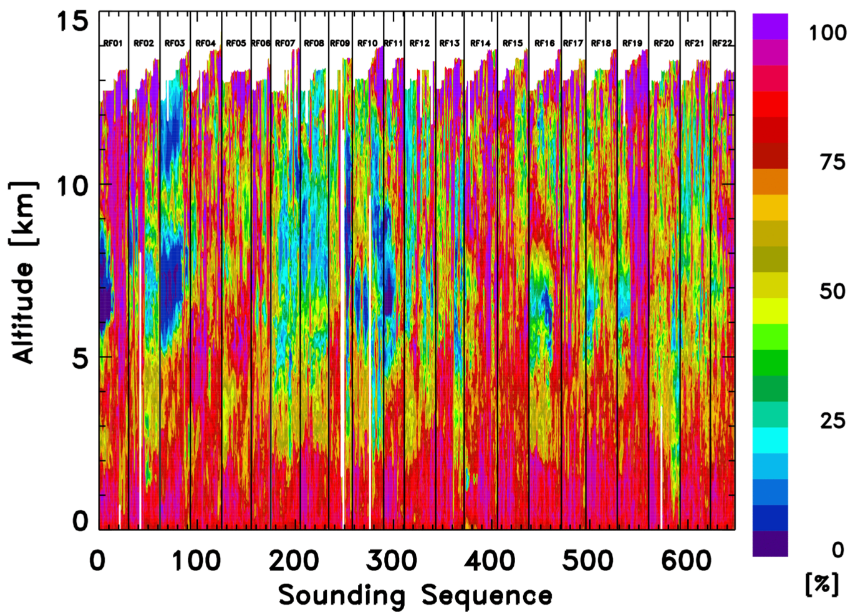

Figure 10: Color contours for all relative humidity measurements. Note that at temperatures below freezing, relative humidity is shown with respect to ice.

7.3 Zonal winds

Zonal wind speeds are shown in Figure 11. Brown colors indicate westerly winds, green and blue colors indicate easterly winds.

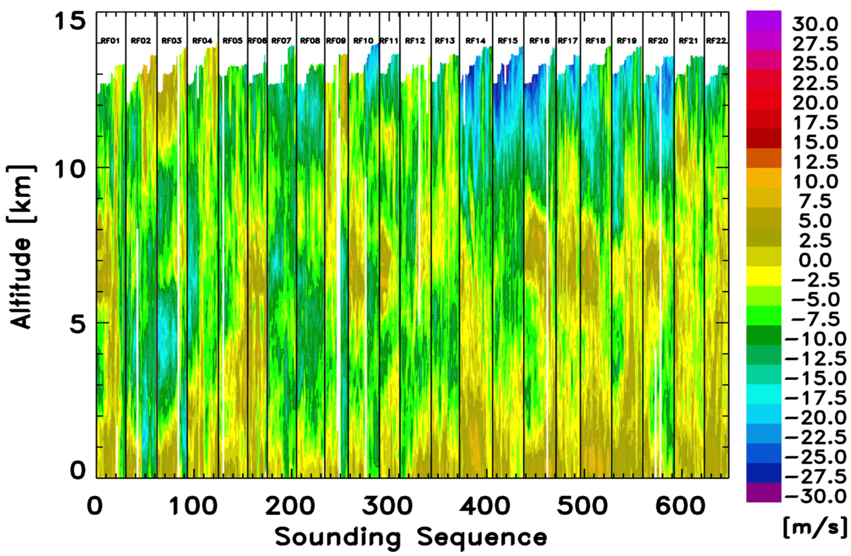

Figure 11: Color contours for all zonal wind speed measurements